

Measurement of $\Upsilon(5S)$ decays to B^0 and B^+ mesons

A. Drutskoy,³ I. Adachi,⁸ H. Aihara,⁴⁴ V. Aulchenko,^{1,33} T. Aushev,^{20,14} A. M. Bakich,³⁹ V. Balagura,¹⁴ V. Bhardwaj,³⁵ M. Bischofberger,²⁶ A. Bondar,^{1,33} A. Bozek,²⁹ M. Bračko,^{22,15} T. E. Browder,⁷ Y. Chao,²⁸ A. Chen,²⁷ P. Chen,²⁸ B. G. Cheon,⁶ S.-K. Choi,⁵ Y. Choi,³⁸ J. Dalseno,^{23,41} M. Danilov,¹⁴ Z. Doležal,² W. Dungel,¹¹ S. Eidelman,^{1,33} N. Gabyshev,^{1,33} B. Golob,^{21,15} H. Ha,¹⁸ J. Haba,⁸ H. Hayashii,²⁶ Y. Horii,⁴³ Y. Hoshi,⁴² W.-S. Hou,²⁸ Y. B. Hsiung,²⁸ H. J. Hyun,¹⁹ T. Iijima,²⁵ K. Inami,²⁵ R. Itoh,⁸ M. Iwabuchi,⁴⁸ Y. Iwasaki,⁸ T. Julius,²⁴ D. H. Kah,¹⁹ J. H. Kang,⁴⁸ N. Katayama,⁸ H. Kichimi,⁸ C. Kiesling,²³ H. J. Kim,¹⁹ H. O. Kim,¹⁹ M. J. Kim,¹⁹ K. Kinoshita,³ B. R. Ko,¹⁸ S. Korpar,^{22,15} P. Krokovny,⁸ T. Kumita,⁴⁵ A. Kuzmin,^{1,33} Y.-J. Kwon,⁴⁸ S.-H. Kyeong,⁴⁸ J. S. Lange,⁴ S.-H. Lee,¹⁸ J. Li,⁷ C. Liu,³⁶ D. Liventsev,¹⁴ R. Louvot,²⁰ A. Matyja,²⁹ S. McOnie,³⁹ K. Miyabayashi,²⁶ H. Miyata,³¹ Y. Miyazaki,²⁵ G. B. Mohanty,⁴⁰ T. Mori,²⁵ R. Mussa,¹³ Y. Nagasaka,⁹ M. Nakao,⁸ Z. Natkaniec,²⁹ S. Nishida,⁸ O. Nitoh,⁴⁶ T. Ohshima,²⁵ S. Okuno,¹⁶ S. L. Olsen,^{37,7} G. Pakhlova,¹⁴ H. Park,¹⁹ H. K. Park,¹⁹ R. Pestotnik,¹⁵ M. Petrič,¹⁵ L. E. Piilonen,⁴⁷ A. Poluektov,^{1,33} S. Ryu,³⁷ Y. Sakai,⁸ O. Schneider,²⁰ C. Schwanda,¹¹ A. J. Schwartz,³ K. Senyo,²⁵ M. E. Sevier,²⁴ M. Shapkin,¹² C. P. Shen,⁷ J.-G. Shiu,²⁸ B. Shwartz,^{1,33} F. Simon,^{23,41} P. Smerkol,¹⁵ S. Stanič,³² M. Starič,¹⁵ K. Sumisawa,⁸ T. Sumiyoshi,⁴⁵ Y. Teramoto,³⁴ K. Trabelsi,⁸ T. Tsuboyama,⁸ Y. Unno,⁶ S. Uno,⁸ Y. Usov,^{1,33} G. Varner,⁷ K. E. Varvell,³⁹ K. Vervink,²⁰ M.-Z. Wang,²⁸ P. Wang,¹⁰ Y. Watanabe,¹⁶ J. Wicht,⁸ E. Won,¹⁸ B. D. Yabsley,³⁹ Y. Yamashita,³⁰ Z. P. Zhang,³⁶ V. Zhulanov,^{1,33} T. Zivko,¹⁵ and A. Zupanc¹⁷

(The Belle Collaboration)

¹*Budker Institute of Nuclear Physics, Novosibirsk*

²*Faculty of Mathematics and Physics, Charles University, Prague*

³*University of Cincinnati, Cincinnati, Ohio 45221*

⁴*Justus-Liebig-Universität Gießen, Gießen*

⁵*Gyeongsang National University, Chinju*

⁶*Hanyang University, Seoul*

⁷*University of Hawaii, Honolulu, Hawaii 96822*

⁸*High Energy Accelerator Research Organization (KEK), Tsukuba*

⁹*Hiroshima Institute of Technology, Hiroshima*

¹⁰*Institute of High Energy Physics, Chinese Academy of Sciences, Beijing*

¹¹*Institute of High Energy Physics, Vienna*

¹²*Institute of High Energy Physics, Protvino*

¹³*INFN - Sezione di Torino, Torino*

¹⁴*Institute for Theoretical and Experimental Physics, Moscow*

¹⁵*J. Stefan Institute, Ljubljana*

¹⁶*Kanagawa University, Yokohama*

¹⁷*Institut für Experimentelle Kernphysik, Karlsruhe Institut für Technologie, Karlsruhe*

¹⁸*Korea University, Seoul*

¹⁹*Kyungpook National University, Taegu*

²⁰*École Polytechnique Fédérale de Lausanne (EPFL), Lausanne*

²¹*Faculty of Mathematics and Physics, University of Ljubljana, Ljubljana*

²²*University of Maribor, Maribor*

²³*Max-Planck-Institut für Physik, München*

²⁴*University of Melbourne, School of Physics, Victoria 3010*

²⁵*Nagoya University, Nagoya*

²⁶*Nara Women's University, Nara*

²⁷*National Central University, Chung-li*

²⁸*Department of Physics, National Taiwan University, Taipei*

²⁹*H. Niewodniczanski Institute of Nuclear Physics, Krakow*

³⁰*Nippon Dental University, Niigata*

³¹*Niigata University, Niigata*

³²*University of Nova Gorica, Nova Gorica*

³³*Novosibirsk State University, Novosibirsk*

³⁴*Osaka City University, Osaka*

³⁵*Panjab University, Chandigarh*

³⁶*University of Science and Technology of China, Hefei*

³⁷Seoul National University, Seoul³⁸Sungkyunkwan University, Suwon³⁹School of Physics, University of Sydney, NSW 2006⁴⁰Tata Institute of Fundamental Research, Mumbai⁴¹Excellence Cluster Universe, Technische Universität München, Garching⁴²Tohoku Gakuin University, Tagajo⁴³Tohoku University, Sendai⁴⁴Department of Physics, University of Tokyo, Tokyo⁴⁵Tokyo Metropolitan University, Tokyo⁴⁶Tokyo University of Agriculture and Technology, Tokyo⁴⁷IPNAS, Virginia Polytechnic Institute and State University, Blacksburg, Virginia 24061⁴⁸Yonsei University, Seoul

Decays of the $\Upsilon(5S)$ resonance to channels with B^+ and B^0 mesons are studied using a 23.6 fb^{-1} data sample collected with the Belle detector at the KEKB asymmetric-energy e^+e^- collider. Fully reconstructed $B^+ \rightarrow J/\psi K^+$, $B^0 \rightarrow J/\psi K^{*0}$, $B^+ \rightarrow \bar{D}^0 \pi^+$ and $B^0 \rightarrow D^- \pi^+$ decays are used to obtain the charged and neutral B production rates per $b\bar{b}$ event, $f(B^+) = (72.1^{+3.9}_{-3.8} \pm 5.0)\%$ and $f(B^0) = (77.0^{+5.8}_{-5.6} \pm 6.1)\%$. Assuming equal rates to B^+ and B^0 mesons in all channels produced at the $\Upsilon(5S)$ energy, we measure the fractions for transitions to two-body and three-body channels with B meson pairs, $f(B\bar{B}) = (5.5^{+1.0}_{-0.9} \pm 0.4)\%$, $f(B\bar{B}^* + B^*\bar{B}) = (13.7 \pm 1.3 \pm 1.1)\%$, $f(B^*\bar{B}^*) = (37.5^{+2.1}_{-1.9} \pm 3.0)\%$, $f(B\bar{B}\pi) = (0.0 \pm 1.2 \pm 0.3)\%$, $f(B\bar{B}^*\pi + B^*\bar{B}\pi) = (7.3^{+2.3}_{-2.1} \pm 0.8)\%$, and $f(B^*\bar{B}^*\pi) = (1.0^{+1.4}_{-1.3} \pm 0.4)\%$. The latter three fractions are obtained assuming isospin conservation.

PACS numbers: 13.25.Gv, 13.25.Hw, 14.40.Pq, 14.40.Nd

New aspects of beauty dynamics can be explored using the large data sample recently collected by Belle at the center-of-mass (CM) energy of the $\Upsilon(5S)$ resonance (also referred to as $\Upsilon(10860)$). Decays of bottomonium states with masses higher than the mass of the $\Upsilon(4S)$ are almost unexplored with only a very limited number of experimental and theoretical studies to date. At the $\Upsilon(5S)$ energy a $b\bar{b}$ quark pair can be produced and hadronize into various final states, which can be classified as two-body B_s^0 ($B_s^0\bar{B}_s^0$, $B_s^0\bar{B}_s^*$, $B_s^*\bar{B}_s^0$, $B_s^*\bar{B}_s^*$) [1, 2], two-body B ($B\bar{B}$, $B\bar{B}^*$, $B^*\bar{B}$, $B^*\bar{B}^*$), three-body ($B\bar{B}\pi$, $B\bar{B}^*\pi$, $B^*\bar{B}\pi$, $B^*\bar{B}^*\pi$), and four-body ($B\bar{B}\pi\pi$) channels. Here B denotes a B^+ or B^0 meson and \bar{B} denotes a B^- or \bar{B}^0 meson. The excited states decay to their ground states via $B^* \rightarrow B\gamma$ and $B_s^* \rightarrow B_s^0\gamma$. Moreover, a $b\bar{b}$ quark pair can also hadronize to a bottomonium state accompanied by π , K or η mesons, for example through a $\Upsilon(5S) \rightarrow \Upsilon(1S)\pi^+\pi^-$ decay [3]. In addition, initial-state radiation (ISR) can affect the final states listed above and must be taken into account [4]. Fractions for all of these channels provide important information about b -quark dynamics.

The first study of B production at the $\Upsilon(5S)$ was performed by CLEO [5, 6] using a 0.42 fb^{-1} data sample. They found the fraction of events with B^{+0} pairs to be $(58.9 \pm 10.0 \pm 9.2)\%$. CLEO interpreted the remaining $(41.1 \pm 10.0 \pm 9.2)\%$ as the fraction of events with B_s^0 mesons. Within the large uncertainties this fraction is 1.6σ larger than the B_s^0 event fraction $f_s = (18.0 \pm 1.3 \pm 3.2)\%$, directly measured by Belle [2]. Both values for this fraction were obtained assuming that contributions from channels with bottomonium states are negligibly small. Among the B^{+0} pair events CLEO found the two-body

fractions for the $B^*\bar{B}^*$ and $B\bar{B}^* + B^*\bar{B}$ channels to be $(74 \pm 15 \pm 8)\%$ and $(24 \pm 9 \pm 3)\%$ [5], respectively. The $B\bar{B}$ channel and multibody channels were not observed and corresponding upper limits were set.

Several theoretical papers have been devoted to $\Upsilon(5S)$ decays to final states with two-body B_s^0 and B^{+0} pairs [7–10]. The $B^*\bar{B}^*$ channel is predicted to be dominant with the fraction over all $b\bar{b}$ events within the range $(30 - 69)\%$ [9, 10]. In these model calculations the other two possible channels have smaller fractions with predictions covering a broad range. Multibody channels have also been theoretically studied [11, 12]; the three-body fractions are found to be about two or three orders of magnitude smaller than the two-body fractions. Interesting information about a possible gluonic component of the $\Upsilon(5S)$ can also be obtained from measurements of the three-body decays [13], if 200 or more events can be reconstructed in a three-body channel.

Here we fully reconstruct the decay modes $B^+ \rightarrow J/\psi K^+$, $B^0 \rightarrow J/\psi K^{*0}$, $B^+ \rightarrow \bar{D}^0 \pi^+$ (using two \bar{D}^0 modes), and $B^0 \rightarrow D^- \pi^+$. Charge-conjugate modes are implicitly included throughout this work. The reconstructed modes have large and precisely measured branching fractions [14] and contain only charged particles.

The data were collected with the Belle detector [15] at KEKB [16], an asymmetric-energy double storage ring e^+e^- collider. This analysis is based on a sample of 23.6 fb^{-1} taken at the $\Upsilon(5S)$ CM energy of $\sim 10867 \text{ MeV}$ and containing $N_{b\bar{b}}^{\Upsilon(5S)} = (7.13 \pm 0.34) \times 10^6$ produced events [2]. The Belle detector is a general-purpose magnetic spectrometer described in detail elsewhere [15].

Charged tracks are assigned as pions or kaons based on

a likelihood ratio $\mathcal{L}_{K/\pi} = \mathcal{L}_K / (\mathcal{L}_K + \mathcal{L}_\pi)$, which includes information obtained from the three Belle particle identification detector subsystems [15]. The identification efficiency for particles used in this analysis varies from 85% to 92% (91% to 98%) for kaons (pions). The electron and muon identification requirements are described in Refs. [17, 18].

The K^{*0} , \bar{D}^0 , D^- and J/ψ candidates are reconstructed in the $K^{*0} \rightarrow K^+\pi^-$, $\bar{D}^0 \rightarrow K^+\pi^-$, $\bar{D}^0 \rightarrow K^+\pi^+\pi^-\pi^-$, $D^- \rightarrow K^+\pi^-\pi^-$, $J/\psi \rightarrow e^+e^-$ and $J/\psi \rightarrow \mu^+\mu^-$ modes. We require the invariant masses to be in the following intervals around the nominal masses: $\pm 50 \text{ MeV}/c^2$ for K^{*0} , $\pm 10 \text{ MeV}/c^2$ for \bar{D}^0 and D^- , $\pm 30 \text{ MeV}/c^2$ for $J/\psi \rightarrow \mu^+\mu^-$, and $^{+30}_{-100} \text{ MeV}/c^2$ for $J/\psi \rightarrow e^+e^-$. A vertex- and mass-constrained fit is applied to J/ψ , \bar{D}^0 and D^- candidates to improve the B signal resolution.

B decays are fully reconstructed and identified using two variables: the energy difference $\Delta E = E_B^{\text{CM}} - E_{\text{beam}}^{\text{CM}}$ and the beam-energy-constrained mass $M_{\text{bc}} = \sqrt{(E_{\text{beam}}^{\text{CM}})^2 - (p_B^{\text{CM}})^2}$, where E_B^{CM} and p_B^{CM} are the energy and momentum of the B candidate in the e^+e^- CM system, and $E_{\text{beam}}^{\text{CM}}$ is the CM beam energy. The intermediate two-body and multibody channels with B^{+0} pairs cluster in distinct regions of the M_{bc} and ΔE plane. However, all channels are distributed along a straight line described approximately by the function $\Delta E = m_B - M_{\text{bc}}$, where m_B is the nominal B mass (fixed to $5.28 \text{ GeV}/c^2$).

After all selections the dominant background is from $e^+e^- \rightarrow q\bar{q}$ continuum events ($q = u, d, s, \text{ or } c$). Events with B mesons tend to be spherical, whereas continuum events are expected to be jet-like. To suppress continuum background, we apply topological cuts. The ratio of the second to the zeroth Fox-Wolfram moments [19] is required to be less than 0.5 for the low background final states with a J/ψ , and less than 0.4 for all others. The angle in the CM between the thrust axis of the particles forming the B candidate and the thrust axis of all other particles in the event, θ_{thr}^* , must satisfy $|\cos \theta_{\text{thr}}^*| < 0.9$ for the final states with a J/ψ , and $|\cos \theta_{\text{thr}}^*| < 0.75$ for all others. More than one B^{+0} candidate per event is allowed, however the probability of multiple candidates is less than 1% for the modes used here, where the final states contain charged particles only.

The two-dimensional M_{bc} and ΔE scatter plots for the $B^+ \rightarrow J/\psi K^+$, $B^0 \rightarrow J/\psi K^{*0}$, $B^+ \rightarrow \bar{D}^0 \pi^+$ ($\bar{D}^0 \rightarrow K^+\pi^-$ and $\bar{D}^0 \rightarrow K^+\pi^+\pi^-\pi^-$) and $B^0 \rightarrow D^-\pi^+$ modes are obtained and are shown in Fig. 1. Events are clearly concentrated along the line $\Delta E = m_B - M_{\text{bc}}$ corresponding to B pair production. The signal regions shown in Fig. 1 are restricted to a $\pm 30 \text{ MeV}$ interval in ΔE (corresponding to $(2.5\text{--}4.0)\sigma$ for the studied modes) and to the kinematically allowed $5.268 \text{ GeV}/c^2 < M_{\text{bc}} < 5.440 \text{ GeV}/c^2$ range. The location of specific channels

within the signal bands will be discussed below and is shown in Fig. 2a.

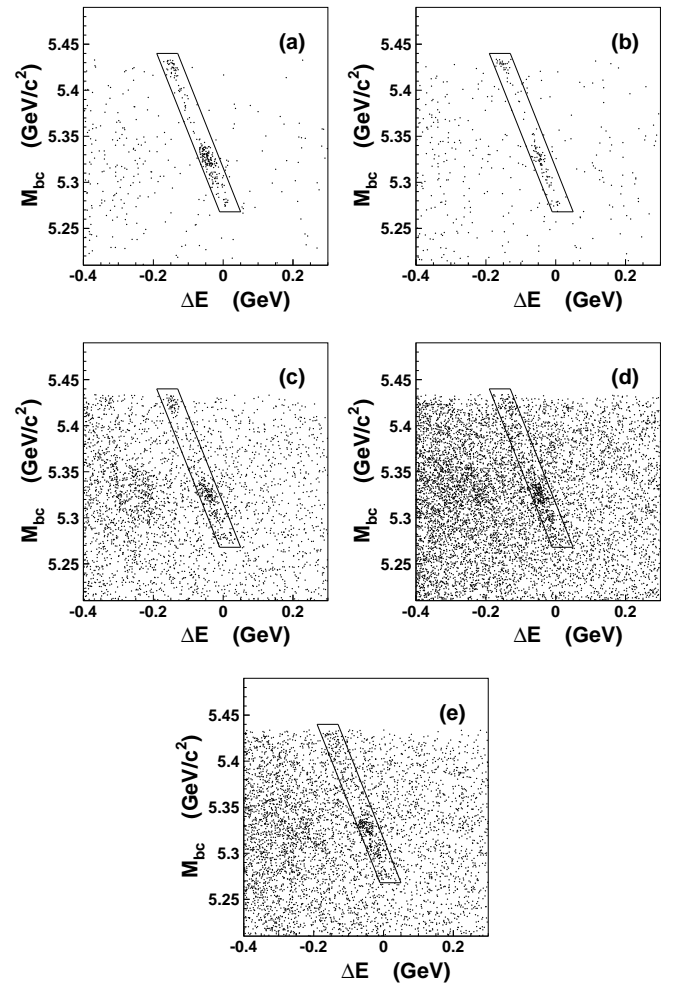


FIG. 1: The M_{bc} and ΔE scatter plots for (a) $B^+ \rightarrow J/\psi K^+$, (b) $B^0 \rightarrow J/\psi K^{*0}$, (c) $B^+ \rightarrow \bar{D}^0(K^+\pi^-)\pi^+$, (d) $B^+ \rightarrow \bar{D}^0(K^+\pi^+\pi^-\pi^-)\pi^+$, and (e) $B^0 \rightarrow D^-\pi^+$ decays. The bands indicate the signal regions corresponding to the intervals $5.268 \text{ GeV}/c^2 < M_{\text{bc}} < 5.440 \text{ GeV}/c^2$ and $|\Delta E + M_{\text{bc}} - m_B| < 0.03 \text{ GeV}$.

We use inclined $\Delta E + M_{\text{bc}} - m_B$ projections of the two-dimensional scatter plots for all events within the range $5.268 \text{ GeV}/c^2 < M_{\text{bc}} < 5.440 \text{ GeV}/c^2$ to obtain integrated B decay event yields. We fit these distributions with a function including two terms: a Gaussian to describe the signal and a first-order polynomial to describe background. The regions where cross-channel B backgrounds can contribute are not used in the fits.

Using the fit results, the charged and neutral B production rates per $b\bar{b}$ event are obtained from the formula:

$$f(B^{+0}) = Y_{B \rightarrow X}^{\text{fit}} / (N_{b\bar{b}}^{\gamma(5S)} \times \epsilon_{B \rightarrow X} \times \mathcal{B}_{B \rightarrow X}), \quad (1)$$

where $Y_{B \rightarrow X}^{\text{fit}}$ is the event yield obtained from the fit for a specific mode $B \rightarrow X$, $\epsilon_{B \rightarrow X}$ is the reconstruction efficiency including intermediate branching fractions, and

$\mathcal{B}_{B \rightarrow X}$ is the corresponding B decay branching fraction [14]. The event yields, efficiencies, and production rates are listed in Table I.

TABLE I: Event yields obtained from fits, efficiencies, and B production rates $f(B^{+/0})$. Efficiencies include intermediate J/ψ , K^{*0} , \bar{D}^0 and D^- branching fractions.

Decay mode	Yield	Efficiency, %	$f(B^{+/0}), \%$
$B^+ \rightarrow J/\psi K^+$	221^{+16}_{-15}	3.41	$89.0^{+6.3}_{-6.1} \pm 8.0$
$B^0 \rightarrow J/\psi K^{*0}$	105 ± 11	1.30	$85.3^{+9.2}_{-8.8} \pm 8.8$
$B^+ \rightarrow \bar{D}^0(K\pi)\pi^+$	215 ± 21	0.97	$64.0 \pm 6.2 \pm 4.9$
$B^+ \rightarrow \bar{D}^0(K3\pi)\pi^+$	275 ± 32	1.17	$68.3^{+8.0}_{-8.1} \pm 6.4$
$B^0 \rightarrow D^- \pi^+$	247 ± 25	1.80	$72.9 \pm 7.4 \pm 6.4$

The systematic uncertainties include those due to the determination of the number of $b\bar{b}$ events (4.7%), charged track reconstruction efficiency (1% per track), particle identification (0.5–1.0% per π and K , 2% per electron, 3% per muon), J/ψ , \bar{D}^0 and D^- mass cut efficiencies (2%), signal and background modeling in the fit procedure (2%), MC statistics in efficiency determination (1–2%), shape of the B meson angular distribution relative to the beam axis direction in the CM system (1%), and PDG branching fractions (3–5%). All systematic uncertainties are combined in quadrature to obtain the total systematic uncertainty. The same set of uncertainties is used below to obtain the total systematic uncertainties for values averaged over several B modes, however the correlated and uncorrelated uncertainties are treated separately in this case. All uncorrelated uncertainties from all B modes are varied individually to obtain their contribution to the total systematic uncertainty of the averaged value, while correlated uncertainties are varied simultaneously for all channels.

Using the rates shown in Table 1, the average production rates $f(B^+) = (72.1^{+3.9}_{-3.8} \pm 5.0)\%$ and $f(B^0) = (77.0^{+5.8}_{-5.6} \pm 6.1)\%$ are obtained. As expected, these rates are equal within uncertainties. The average of charged and neutral B modes is $(73.7 \pm 3.2 \pm 5.1)\%$. Within uncertainties this rate is consistent with the CLEO value of $(58.9 \pm 10.0 \pm 9.2)\%$ [6].

Since the $f(B^+)$ and $f(B^0)$ values are consistent with isospin symmetry, it is reasonable to assume that equal numbers of B^+ and B^0 mesons are produced in all possible channels. Therefore the five B decay modes are treated simultaneously everywhere below. First, events in the signal bands shown in Fig. 1 are projected onto M_{bc} . To describe combinatorial backgrounds under the signal, we define sidebands, which have the same shape as the signal region, but are shifted by ± 70 MeV in ΔE , and project similarly onto M_{bc} . Assuming that background is distributed linearly in ΔE , we model the combinatorial background by taking the average of the two sideband M_{bc} distributions.

Figure 2(a) shows the M_{bc} distributions for the pos-

sible two-, three- and four-body channels obtained from MC simulation for the $B^0 \rightarrow D^- \pi^+$ decay. The three-body and four-body channels are simulated assuming a pure phase-space decay model. Figure 2(a) shows that the two-body channels are well separated. The three-body $B\bar{B}\pi$, $B\bar{B}^*\pi + B^*\bar{B}\pi$ and $B^*\bar{B}^*\pi$ channels have broader distributions in the higher mass region $M_{bc} > 5.35$ GeV/ c^2 . The four-body $B\bar{B}\pi\pi$ channel is the cross-hatched peak on the right side of Fig. 2(a).

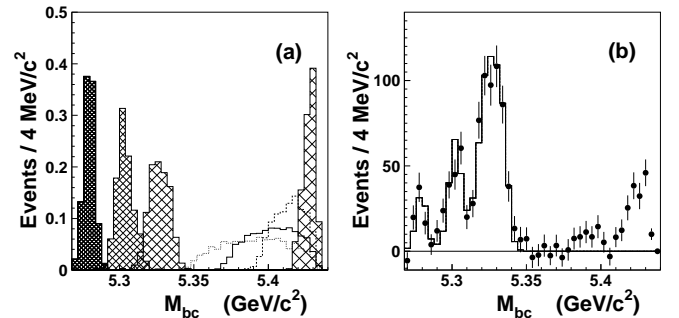


FIG. 2: (a) MC simulated M_{bc} distributions for the $B^0 \rightarrow D^- \pi^+$ decay for $B\bar{B}$, $B\bar{B}^* + B^*\bar{B}$, $B^*\bar{B}^*$ and $B\bar{B}\pi\pi$ channels (cross-hatched histograms from left to right), and also for the three-body channels $B\bar{B}^*\pi + B^*\bar{B}\pi$ (plain histogram), $B\bar{B}\pi$ (dotted) and $B^*\bar{B}^*\pi$ (dashed). The distributions are normalized to unity. (b) M_{bc} distribution in data after background subtraction. The sum of the five studied B decays (points with error bars) and results of the fit (histogram) used to extract the two-body channel fractions are shown. The fitting procedure is described in the text.

The matrix elements responsible for the three- and four-body decays are not known, and the rates of the three- and four-body contributions cannot be obtained in a model-independent way from a fit to these M_{bc} distributions. We therefore restrict the fit to the region 5.268 GeV/ $c^2 < M_{bc} < 5.348$ GeV/ c^2 to extract the two-body channel fractions. To obtain the sum of the other contributions in the large M_{bc} region, only the events from the interval 5.348 GeV/ $c^2 < M_{bc} < 5.440$ GeV/ c^2 are selected. For these distributions we apply a fit procedure similar to that used above to obtain the full $f(B^{+/0})$ production rate for the entire interval 5.268 GeV/ $c^2 < M_{bc} < 5.440$ GeV/ c^2 . The total signal yield, summed over all modes and channels in this region, is $228.7^{+22.9}_{-22.3}$.

The fitting procedure used to extract the production rates of the two-body decay channels treats the five signal and five sideband M_{bc} distributions simultaneously. The following four components with fixed shapes and floating normalizations are included in the fit for each distribution: $B\bar{B}$, $B\bar{B}^* + B^*\bar{B}$, $B^*\bar{B}^*$, and combinatorial background. The shapes of the signal components are taken from MC simulation, and those of combinatorial background are modeled by the sideband data. The normalization parameters (channel fractions) for the two-body components are constrained to be equal for all five stud-

ied B decays. The sum of background-subtracted M_{bc} distributions for the five studied B decays is shown in Fig. 2(b), where the result of the likelihood fit in the region $5.268 \text{ GeV}/c^2 < M_{bc} < 5.348 \text{ GeV}/c^2$ used to obtain two-body channel fractions is superimposed. The fractions obtained from the fit are listed in Table II. The systematic uncertainties include all those described above as well as uncertainties due to the M_{bc} signal shape modeling (3%).

TABLE II: The fractions of two-body channels with B^+ and B^0 mesons. The fraction obtained from a fit to the large M_{bc} region is also given.

Channel	Fraction, %
$B\bar{B}$	$5.5^{+1.0}_{-0.9} \pm 0.4$
$B\bar{B}^* + B^*\bar{B}$	$13.7 \pm 1.3 \pm 1.1$
$B^*\bar{B}^*$	$37.5^{+2.1}_{-1.9} \pm 3.0$
Large M_{bc}	$17.5^{+1.8}_{-1.6} \pm 1.3$

To reconstruct the three-body channels, we look for an additional charged pion produced directly in the $B^{(*)}\bar{B}^{(*)}\pi^+$ channels. For each charged pion not included in the reconstructed B candidate, we form right-sign $B^+\pi^-$, $\bar{B}^0\pi^-$, $B^0\pi^+$ or $B^-\pi^+$ combinations. We then compute the variables M_{bc}^{mis} and ΔE^{mis} for the missing B meson, using the energy and momentum of the reconstructed $B\pi$ combination in the CM: $E(B^{\text{mis}}) = 2E_{\text{beam}}^{\text{CM}} - E(B\pi)^{\text{CM}}$ and $p(B^{\text{mis}}) = p(B\pi)^{\text{CM}}$. In the $B\bar{B}^*\pi^+ + B^*\bar{B}\pi^+$ and $B^*\bar{B}^*\pi^+$ channels, the ΔE^{mis} value will be shifted due to unreconstructed photons from B^* decays.

Figure 3(a) shows the corrected $\Delta E^{\text{mis}} + M_{bc}^{\text{mis}} - m_B$ projections for MC simulated $B\bar{B}\pi^+$, $B\bar{B}^*\pi^+ + B^*\bar{B}\pi^+$, $B^*\bar{B}^*\pi^+$, and $B\bar{B}\pi\pi$ events where the $B^+ \rightarrow J/\psi K^+$ mode is generated. The reconstructed B candidates are selected from the signal region within the intervals $5.37 \text{ GeV}/c^2 < M_{bc} < 5.44 \text{ GeV}/c^2$ and $|\Delta E + M_{bc} - m_B| < 0.03 \text{ GeV}$. The value $\Delta E^{\text{mis}} + M_{bc}^{\text{mis}} - m_B$ is corrected by adding to it the value $\Delta E + M_{bc} - m_B$. This does not introduce any bias for the original B mesons, but improves the resolution, because these two values have partially anticorrelated uncertainties. Figure 3a shows that the $B\bar{B}\pi^+$, $B\bar{B}^*\pi^+ + B^*\bar{B}\pi^+$ and $B^*\bar{B}^*\pi^+$ channel contributions are well separated. The reconstruction efficiency for the four-body channel (the small peak in the rightmost part of Fig. 3(a)) is small and model dependent. Therefore, we do not include the four-body channel in the fit procedure described below. The background due to random charged tracks from the unobserved \bar{B} meson is also shown.

Finally, the $\Delta E^{\text{mis}} + M_{bc}^{\text{mis}} - m_B$ distribution is obtained in data for the sum of the five reconstructed \bar{B} modes (Fig. 3(b)). We fit this distribution with a function including four terms: three Gaussians with fixed

shapes and free normalizations to describe the $B\bar{B}\pi^+$, $B\bar{B}^*\pi^+ + B^*\bar{B}\pi^+$, and $B^*\bar{B}^*\pi^+$ contributions, and a second-order polynomial to describe the background. The central positions and widths of the Gaussians are obtained from fits to the MC simulated distributions shown in Fig. 3(a) and are fixed in the fit to data.

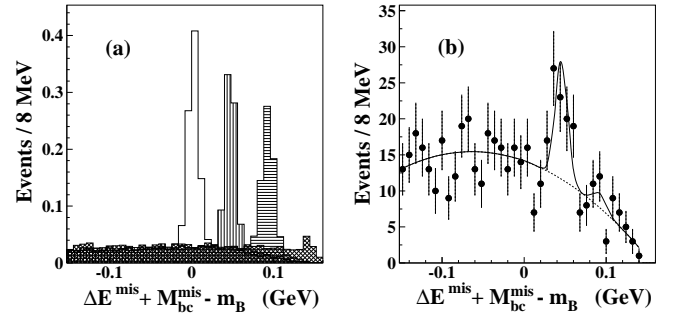


FIG. 3: (a) The $\Delta E^{\text{mis}} + M_{bc}^{\text{mis}} - m_B$ distribution normalized per reconstructed B meson from the MC simulated $B^+ \rightarrow J/\psi K^+$ decays in the (peaks from left to right) $B\bar{B}\pi^+$, $B\bar{B}^*\pi^+ + B^*\bar{B}\pi^+$, $B^*\bar{B}^*\pi^+$, and $B\bar{B}\pi\pi$ channels. (b) The $\Delta E^{\text{mis}} + M_{bc}^{\text{mis}} - m_B$ data distribution for right-sign $B^{-/0}\pi^+$ combinations for all five studied B modes. The curve shows the result of the fit described in the text.

The event yields and rates are listed in Table III. The three-body rates are calculated assuming the ratio of charged and neutral directly produced pions to be 2:1 as expected from isospin conservation. The pion reconstruction efficiencies are obtained from the three-body phase-space matrix element MC simulation to be 73.8%, 64.2% and 57.2% for the $B\bar{B}\pi^+$, $B\bar{B}^*\pi^+ + B^*\bar{B}\pi^+$, and $B^*\bar{B}^*\pi^+$ channels, respectively. In neutral B modes, an efficiency correction is applied to take into account the effect of 19% $B^0 - \bar{B}^0$ mixing. The systematic uncertainties due to the fit procedure (± 1.5 signal events for each channel) and MC efficiency calculations (4–10%) are also included in the total systematic uncertainties. The statistical significance of the $B\bar{B}^*\pi^+ + B^*\bar{B}\pi^+$ signal is 4.4σ .

It is interesting to note that by directly reconstructing pions, we observe only about one half of the rate obtained above for the large M_{bc} region (Table II) resulting in a deficit of $(9.2^{+3.0}_{-2.8} \pm 1.0)\%$. If the difference were due to $B\bar{B}\pi\pi$ events, we would expect 4 ± 2 events in the three rightmost bins of the $\Delta E^{\text{mis}} + M_{bc}^{\text{mis}} - m_B$ distribution of Fig. 3(b), where only one is observed. In addition, the four-body channel is theoretically expected to have a rate at least an order of magnitude smaller than the three-body channel rates, because there is limited phase-space for the creation of an additional pion. Instead, we find that the deficit can be explained by ISR contributions such as $e^+e^- \rightarrow \Upsilon(4S)\gamma \rightarrow B\bar{B}\gamma$. We calculate a probability of $\sim 10\%$ for hard photon emission [4] by the electron or positron beam with subsequent B production, and estimate that $\sim 40\%$ of such events are due to radiative return to the $\Upsilon(4S)$ resonance. This esti-

mate agrees with the observed residual and explains the peaking structure on the right side of Fig. 2(b), which is dominated by radiative return to the $\Upsilon(4S)$ or slightly higher energies.

TABLE III: The three-body channel yields and fractions. The yields are obtained from a fit to the $\Delta E^{\text{mis}} + M_{bc}^{\text{mis}} - m_B$ distribution using five studied B decay modes. The sum of the large M_{bc} channel rates is taken from Table II. The residual is the difference between the sum of the three-body channels and the result from the large M_{bc} region.

Channel	Yield (π^+), events	Fraction over large M_{bc} %	Fraction per $b\bar{b}$ event %
$B\bar{B}\pi$	$0.2^{+7.2}_{-6.9}$	$0.2^{+6.8}_{-6.5}$	$0.0 \pm 1.2 \pm 0.3$
$B\bar{B}^*\pi + B^*\bar{B}\pi$	$38.3^{+10.5}_{-9.8}$	$41.6^{+12.1}_{-11.4}$	$7.3^{+2.3}_{-2.1} \pm 0.8$
$B^*\bar{B}^*\pi$	$4.8^{+6.4}_{-5.9}$	$5.9^{+7.8}_{-7.2}$	$1.0^{+1.4}_{-1.3} \pm 0.4$
Residual		$52.3^{+15.9}_{-15.0}$	$9.2^{+3.0}_{-2.8} \pm 1.0$
Large M_{bc}		100.	$17.5^{+1.8}_{-1.6} \pm 1.3$

We analyze other potential sources and backgrounds for the events in the multibody region. The rate for a $b\bar{b}$ event to produce the $\Upsilon(4S)$ and two pions is expected to be less than 1% [3]. The wide $J^P = 1^+ B^{**}$ meson can be produced at the $\Upsilon(5S)$ CM energy with a subsequent decay resulting in three- or four-body channels, however this process is expected to be negligible due to the very small phase-space. The decay $B_s^0 \rightarrow B^+ e^- \bar{\nu}_e$ could contribute as a background to the multibody channels, however, the corresponding branching fraction is estimated to be less than 10^{-4} .

In conclusion, the production of B^+ and B^0 mesons is measured at the energy of the $\Upsilon(5S)$. Using fully reconstructed B^+ and B^0 mesons the production rates per $b\bar{b}$ event are measured to be $f(B^+) = (72.1^{+3.9}_{-3.8} \pm 5.0)\%$ and $f(B^0) = (77.0^{+5.8}_{-5.6} \pm 6.1)\%$. The average value $(73.7 \pm 3.2 \pm 5.1)\%$ agrees within uncertainties with the CLEO value of $(58.9 \pm 10.0 \pm 9.2)\%$ [6]. Taking into account the $B_s^{(*)}\bar{B}_s^{(*)}$ event rate at the $\Upsilon(5S)$ of $f_s = (19.5^{+3.0}_{-2.2})\%$ [14] (this value was obtained neglecting bottomonium, resulting in an additional absolute uncertainty of about 1%), and assuming the fraction of final states with a bottomonium meson to be $1 - f(B^+)/2 - f(B^0)/2 - f_s$, some room for unobserved transitions still remains.

Assuming equal production of B^+ and B^0 mesons we also measure the fractions for $b\bar{b}$ event transitions to the two-body channels with B^{+0} meson pairs, $f(B\bar{B}) = (5.5^{+1.0}_{-0.9} \pm 0.4)\%$, $f(B\bar{B}^* + B^*\bar{B}) = (13.7 \pm 1.3 \pm 1.1)\%$, $f(B^*\bar{B}^*) = (37.5^{+2.1}_{-1.9} \pm 3.0)\%$. The $B\bar{B}$ channel is measured for the first time. These fractions are in rough agreement with theoretical predictions [9, 10], however further adjustment of the theoretical models is required.

Using the additional charged pion directly produced in $B^{(*)}\bar{B}^{(*)}\pi^+$ channels, we measure the three-body channel fractions in a model-dependent way. The $B\bar{B}^*\pi +$

$B^*\bar{B}\pi$ decay channel is observed for the first time with the fraction $f(B\bar{B}^*\pi + B^*\bar{B}\pi) = (7.3^{+2.3}_{-2.1} \pm 0.8)\%$. This measured three-body fraction is significantly larger than those predicted in [11, 12].

We thank the KEKB group for the excellent operation of the accelerator, the KEK cryogenics group for the efficient operation of the solenoid, and the KEK computer group and the National Institute of Informatics for valuable computing and SINET3 network support. We acknowledge support from the Ministry of Education, Culture, Sports, Science, and Technology (MEXT) of Japan, the Japan Society for the Promotion of Science (JSPS), and the Tau-Lepton Physics Research Center of Nagoya University; the Australian Research Council and the Australian Department of Industry, Innovation, Science and Research; the National Natural Science Foundation of China under contract No. 10575109, 10775142, 10875115 and 10825524; the Ministry of Education, Youth and Sports of the Czech Republic under contract No. LA10033 and MSM0021620859; the Department of Science and Technology of India; the BK21 and WCU program of the Ministry Education Science and Technology, National Research Foundation of Korea, and NSDC of the Korea Institute of Science and Technology Information; the Polish Ministry of Science and Higher Education; the Ministry of Education and Science of the Russian Federation and the Russian Federal Agency for Atomic Energy; the Slovenian Research Agency; the Swiss National Science Foundation; the National Science Council and the Ministry of Education of Taiwan; and the U.S. Department of Energy. This work is supported by a Grant-in-Aid from MEXT for Science Research in a Priority Area (“New Development of Flavor Physics”), and from JSPS for Creative Scientific Research (“Evolution of Tau-lepton Physics”).

-
- [1] M. Artuso *et al.* (CLEO Collaboration), Phys. Rev. Lett. **95**, 261801 (2005).
 - [2] A. Drutskoy *et al.* (Belle Collaboration), Phys. Rev. Lett. **98**, 052001 (2007).
 - [3] K.-F. Chen *et al.* (Belle Collaboration), Phys. Rev. Lett. **100**, 112001 (2008).
 - [4] M. Benayoun *et al.*, Mod. Phys. Lett. A **14**, 2605 (1999).
 - [5] O. Aquines *et al.* (CLEO Collaboration), Phys. Rev. Lett. **96**, 152001 (2006).
 - [6] G. S. Huang *et al.* (CLEO Collaboration), Phys. Rev. D **75**, 012002 (2007).
 - [7] N. A. Tornqvist, Phys. Rev. Lett. **53**, 878 (1984).
 - [8] S. Ono, A. I. Sanda, and N. A. Tornqvist, Phys. Rev. D **34**, 186 (1986).
 - [9] Yu. A. Simonov and A. I. Veselov, Phys. Lett. B **671**, 55 (2009).
 - [10] D. S. Hwang and H. Son, arXiv:0812.4402 [hep-ph].
 - [11] Yu. A. Simonov and A. I. Veselov, JETP Lett. **88**, 5 (2008).

- [12] L. Lellouch, L. Randall, and E. Sather, Nucl. Phys. B **405**, 55 (1993).
- [13] I. J. General, S. R. Cotanch, and F. J. Llanes-Estrada, Eur. Phys. J. C **51**, 347 (2007).
- [14] C. Amsler *et al.* (Particle Data Group), Phys. Lett. B **667**, 1 (2008).
- [15] A. Abashian *et al.* (Belle Collaboration), Nucl. Instr. and Meth. A **479**, 117 (2002).
- [16] S. Kurokawa and E. Kikutani, Nucl. Instr. and Meth. A **499**, 1 (2003), and other papers included in this Volume.
- [17] K. Hanagaki *et al.*, Nucl. Instr. and Meth. A **485**, 490 (2002).
- [18] A. Abashian *et al.*, Nucl. Instr. and Meth. A **491**, 69 (2002).
- [19] G. C. Fox and S. Wolfram, Phys. Rev. Lett. **41**, 1581 (1978).